

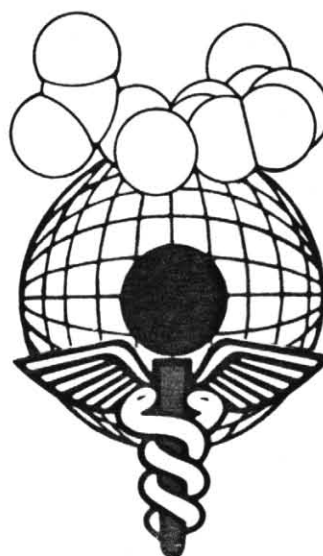
Visualization in Biomedical Computing 1992

Richard A. Robb
Editor

13-16 October 1992
Chapel Hill, North Carolina

Sponsored by
The Computer Science Department
of the University of North Carolina at Chapel Hill

In cooperation with
The Alliance for Engineering in Medicine & Biology
The American Association of Physicists in Medicine
Computer Assisted Radiology
IEEE Engineering in Medicine & Biology Society
IEEE Computer Society, Technical Committee on Graphics
The International Federation for Medical And Biological Engineering
SPIE—The International Society for Optical Engineering



Volume 1808

Wavelet Processing Techniques for Digital Mammography

Andrew Laine and Shuwu Song

Computer and Information Sciences Department
University of Florida, Gainesville, FL 32611
Email: laine@cis.ufl.edu, Phone: (904) 392-1239

Abstract

This paper introduces a novel approach for accomplishing mammographic feature analysis through multiresolution representations. We show that efficient (nonredundant) representations may be identified from digital mammography and used to enhance specific mammographic features within a continuum of scale space. The multiresolution decomposition of wavelet transforms provides a natural hierarchy in which to embed an interactive paradigm for accomplishing scale space feature analysis. Similar to traditional coarse to fine matching strategies, the radiologist may first choose to look for coarse features (e.g. dominant mass) within low frequency levels of a wavelet transform and later examine finer features (e.g. microcalcifications) at higher frequency levels. In addition, features may be extracted by applying geometric constraints within each level of the transform. Choosing wavelets (or analyzing functions) that are simultaneously localized in both space and frequency, results in a powerful methodology for image analysis. Multiresolution and orientation selectivity, known biological mechanisms in primate vision, are ingrained in wavelet representations and inspire the techniques presented in this paper.

Our approach includes local analysis of complete multiscale representations. Mammograms are reconstructed from wavelet representations, enhanced by linear, exponential and constant weight functions through scale space. By improving the visualization of breast pathology we can improve the chances of early detection of breast cancers (improve quality) while requiring less time to evaluate mammograms for most patients (lower costs).

1. Introduction

Many cancers escape detection due to the density of surrounding breast tissue. For example, differences in attenuation of the various soft tissue structures in the female breast are small, and it is necessary to use low levels of X-ray energy to obtain high contrast in mammographic film. Since contrast between the soft tissues of the breast is inherently low and because relatively minor changes in mammary structure can signify the presence of a malignant breast tumor, the detection is more difficult in mammography than in most other forms of radiography. The radiologist must search for malignancy in mammographic features such as microcalcifications, dominate and stellate masses, as well as textures of fibrous tissues.

A primary breast carcinoma can metastasize when it consists of a relatively small number of cells, far below our present threshold of detection. The importance of diagnosis of breast cancer at an early stage is critical to patient survival. The cure rate for breast lesions of 0.5cm or less in diameter can approach 100%. Despite advances and improvements in mammography and mammographic screening programs, the detection of minimal breast cancer (those cancers 1.0cm or less in diameter) remains difficult. At present, mammography is capable of detecting some cases through indirect signs, particularly through the presence of characteristic microcalcifications. It has been suggested that as normally viewed, *mammograms display only about 3% of the information they detect!* The inability to detect these small tumors motivates the imaging techniques and methods of analysis presented in this paper.

Digital image processing techniques have been applied previously mammography. The focus of past investigations has been to enhance mammographic features while reducing the enhancement of noise. Gordon and Rangayyan[14] used an adaptive neighborhood image processing to enhance the contrast of selected features relevant to mammography. This method enhanced the contrast of mammographic features as well as noise and digitization effects. Dhawan[11][12][13] have made significant contributions towards solving problems encountered in mammographic image enhancement. Dhawan developed an adaptive neighborhood-based image processing technique that utilized low-level analysis and knowledge about a desired feature in the design of a contrast enhancement function to improve the contrast of specific features. They found that a suitable contrast enhancement function is useful but difficult to design. Dhawan and Le Royer [13] developed a method which defined an adaptive neighborhood and used a global model to compute the best contrast enhancement function based on *a priori* knowledge of specific types of mammographic features. These results provided an algorithm that was very

efficient and "tunable" in many aspects to enhance relevant diagnostic information with little or no enhancement of noise. Recently, Tahoces [25] developed a method for the enhancement of chest and breast radiographies by automatic spatial filtering. In their method, they used a linear combination of an original image and two smoothed images obtained from the original image by applying different spatial masks. The process was completed by nonlinear contrast stretching. This spatial filtering enhanced edges while minimally amplifying noise.

Recent approaches to automate the detection of tumors in mammograms have relied on some method of feature enhancement. Brzakovic [2] developed an automated system for the detection and classification of particular types of tumors in digitized mammograms based on tumor features. They used a threshold parameter and a fuzzy pyramid link to identify homogenous regions and then applied a second threshold to separate selected regions from the background.

Methods of feature enhancement have been key to the success of classification algorithms. Lai [15] compared several image enhancement methods for detecting circumscribed masses in mammograms. They compared an edge-preserving smoothing function [23], a half-neighborhood method [24], k-nearest neighborhood, directional smoothing [9] and median filtering [1] and in addition proposed a method of selective median filtering. In this method, the median was restricted to those pixels having a difference in gray level intensity from the central pixel no larger than some threshold within its neighborhood. Among the five techniques implemented, they concluded that selective median filtering with a 5×5 neighborhood performed best for image enhancement and noise-cleaning.

In the fields of image processing and computer vision, transforms such as windowed Fourier transforms that can decompose a signal into a set of frequency intervals of constant size have been applied to many applications, including image compression and texture analysis. Because the spatial and frequency resolutions of these transforms remain fixed, the information provided by such transforms is not local within each interval. A wavelet transform [19][18] [20][21][7][8] is a decomposition of a signal onto a family of functions called a wavelet family. It decomposes an image onto a set of frequency channels having a constant bandwidth in logarithmic scale and overcomes many drawbacks of windowed Fourier methods. The wavelet transform gives a precise understanding of the concept of multiresolution, which has been widely used in signal processing and harmonic analysis. In wavelet analysis, the variation of resolution enables the transform to focus on irregularities of a signal and characterize them locally. Wavelet transforms can not only detect sharp variations of a signal but may also characterize their local shape.

In this paper we propose a novel method for accomplishing feature enhancement [16]. Two complete image representations are engaged: coefficients from a dyadic wavelet transform and wavelet maxima coefficients [22]. We demonstrate how to emphasize distinct features in a mammogram by modifying these representations for improved visualization of breast pathology.

In the following section we present a description of a wavelet transform and its properties. In section 3, we introduce several enhancement techniques based on wavelet representations. Preliminary results of our enhancement methods are presented in section 4. Finally, in section 5, we summarize our results and discuss future directions of research.

2. A Framework for Multiscale Analysis

In this paper, we accomplish mammographic feature analysis through a novel method of multiresolution representation. We shall demonstrate that efficient (nonredundant) representations may be identified from digital mammography and used to reconstruct mammographic features within a continuum of scale space. Such reconstructions can complement existing modalities and *allow a radiologist to examine interactively emergent features within a selected scale space*. In addition, we suggest that these representations may increase the capacity and reliability of autonomous systems to accomplish classification of known abnormalities.

The novelty of our approach includes the application of wavelet transforms to accomplish scale space feature analysis and detection. The wavelet transform, introduced by Lemarie and Meyer (1986) [17] has received considerable attention in the mathematical and signal processing communities. Using wavelets as a set of basis functions, we may decompose an image into a multiresolution hierarchy of localized information at different spatial frequencies. Wavelet bases are more attractive than traditional hierarchical bases because they are orthonormal, linear, continuous, and continuously invertible. The multi-scale representation of wavelet transforms suggest a mathematically coherent basis not only for existing multi-grid techniques, but also for embedding new methods. For example, wavelet transforms may be used to integrate sparse data, resolve ambiguities in optic flow fields, accomplish fast surface interpolation, and image compression [10].

In contrast to ad-hoc approaches, our method suggests the development of a practical diagnostic tool embedded in a unified mathematical theory. By this virtue, wavelet methods can exceed the performance of previous multiresolution techniques that have relied mostly on traditional methods of time-frequency analysis such as the Wigner distribution (1932) and Gabor's sliding-window (1946) transforms.

The multiresolution decomposition of wavelet transforms provides a natural hierarchy in which to embed an interactive paradigm for accomplishing scale space feature analysis. Similar to traditional coarse to fine matching strategies, the radiologist may first choose to look for coarse features (e.g. dominant masses) within low frequency levels of the wavelet transform and later examine finer features (e.g. microcalcifications) at higher frequency levels. Choosing wavelets (or analyzing functions) that are simultaneously localized in both space and frequency, results in a powerful methodology for image analysis. The inner-product of a signal f with a wavelet Ψ ($\langle f, \Psi \rangle = (2\pi)^{-1} \langle \hat{f}, \hat{\Psi} \rangle$) reflects the character of f within the time-frequency region where Ψ is localized ($\hat{\Psi}$ and \hat{f} are the Fourier transforms of the analyzing function Ψ and the signal f). If Ψ is spatially localized, then 2-D features such as shape and orientation are preserved in the transform space and may characterize a feature through scale space. We may "extract" such features by applying geometric constraints within each level of the wavelet transform. We reduce the complexity of the reconstructed mammogram by selecting a subset of features that satisfy certain geometric constraints. For example, we may choose to focus on only those features oriented in the horizontal direction. Subsequent image reconstructions may use the context provided by previously enhanced features to examine (diagnose) additional features emergent at other scales and orientations. Thus, fine vertical features may be selected and analyzed in the context of previously classified large horizontal features. Our strategy provides a global context upon which subtle features within finer scales may be classified incrementally through a precomputed hierarchy of wavelet dilations.

Our approach to feature analysis and classification is motivated in part by recently discovered biological mechanisms of the human visual system. Both multiorientation and multiresolution are features of the human visual system. There exist cortical neurons which respond specifically to stimuli within certain orientations and frequencies. In 1989, Nobel laureate Wiesel demonstrated orientation selectivity in Area 17 of the visual cortex where binocular neurons (stereo) had been previously mapped[3].

Wavelet decompositions provide a natural way to manipulate image features. A wavelet decomposition breaks down a signal $f(x)$ into a family of functions that are the translations and dilations of a function $\Psi(x)$ called a wavelet. From the Fourier transform of a wavelet and its dilations we know that the passing bands for the dilations of a wavelet are the same on a logarithmic scale for all scaling factors. Hence a wavelet transform decomposes a signal onto a set of frequency bands of constant size on a logarithmic scale. Another important property of the wavelet transform is that the local regularity of a signal (or the type of local singularity) can be characterized by the transform coefficients.

In this paper we show how these properties can be used for enhancement in digital mammography. In practice we choose a special set of scaling factors and exploit the mathematical properties of wavelets (including linearity, continuity, continuous invertibility) to make features more obvious. A wavelet transform depends on two parameters s and x which vary continuously over the set of real numbers. If the scale parameter s is sampled along the dyadic sequence $[2^j]_{j \in \mathbb{Z}}$, we generate a wavelet family of functions $\Psi_{2^j}(x)$. The dyadic wavelet transform of a function $f(x)$: $[W_{2^j} f(x)]_{j \in \mathbb{Z}}$ may be denoted by

$$Wf = [W_{2^j} f(x)]_{j \in \mathbb{Z}}.$$

A function $f(x)$ can be reconstructed from its dyadic wavelet transform,

$$f(x) = \sum_{j=-\infty}^{+\infty} W_{2^j} f(x) * \Psi_{2^j}(-x)$$

and denoted by

$$f(x) = W^{-1}[Wf(x)].$$

Let V be the space of dyadic wavelet transforms $[W_{2^j} f(x)]_{j \in \mathbb{Z}}$ for all functions $f(x) \in L^2(\mathbb{R})$. If V is a subspace of $l^2(L^2)$, then W^{-1} is an operator from $l^2(L^2)$ to $L^2(\mathbb{R})$ and $P_V = W \bullet W^{-1}$ is a projector from $l^2(L^2)$ onto the space V .

As mentioned above, wavelet transforms can be used to characterize the type of local singularities of a signal. While the maxima of a wavelet transform can be used to detect signal peaks (edges). The local maxima of a wavelet transform

detects a signals' acute variations and characterizes their local shape. The local maxima defines a stable representation of an original signal. A slight perturbation of a signal will not change the position of its local maxima. The completeness of the representation can be shown by the reconstruction of a signal from its wavelet maxima alone.

It is easy to show that $f(x)$ can be recovered from its dyadic wavelet transform[21]. We first reconstruct $[W_{2^j}f(x)]_{j \in \mathbb{Z}}$ from the local maxima of each function $W_{2^j}f(x)$. For any scale 2^j there exists an infinite number of functions $g_j(x)$ which have the same local maxima as $W_{2^j}f(x)$. However any sequence of functions $g_j(x)$ is not necessarily a dyadic wavelet transform of some function in $L^2(\mathbb{R})$. Of these sequences of functions, a function that satisfies the reproducing kernel conditions of a dyadic wavelet is the dyadic wavelet transform. The set Γ of all sequences $(g_j)_{j \in \mathbb{Z}}$ in $l^2(L^2)$ is defined such that for all scales 2^j , $g_j(x) \in H^1(\mathbb{R})$, $g_j(x)$ has the same maxima as $W_{2^j}f(x)$.

A classical technique for recovering the intersection of a convex set Γ with a linear space V is to iterate on alternative projections on the convex and linear space[22]. Suppose Γ is closed in Hilbert space, we can define a projection P_Γ on Γ that transforms $[g_j(x)]_{j \in \mathbb{Z}}$ into the sequence of functions $[h_j(x)]_{j \in \mathbb{Z}} \in \Gamma$ that is closest to $[g_j(x)]_{j \in \mathbb{Z}}$. The set Γ is convex so the projection P_Γ is not expansive. P_V is an orthogonal projection on the space V . The intersection of Γ and V is a fixed point, which may be computed by iteration on the operator P , $P = P_\Gamma \bullet P_V$. We can show that for any sequence of functions $[g_j(x)]_{j \in \mathbb{Z}}$, as n tends to positive infinity $P^{(n)}[g_j(x)]_{j \in \mathbb{Z}}$ converges weakly to an element in the intersection of Γ and V . This element is the dyadic wavelet transform of $f(x)$.

3. Local Enhancement Techniques

In the case of two-dimensional signals (images), we can define a two-dimensional wavelet $\Psi^k(x, y)$, and its wavelet transform by

$$W_{2^j}^k f(x, y) = f(x, y) * \frac{1}{2^j} \Psi^k\left(\frac{x}{2^j}, \frac{y}{2^j}\right) \quad k = 1, \dots, K, \quad K \in \mathbb{Z}^+$$

$$f(x, y) = \sum_{k=1}^K \sum_{j=-\infty}^{+\infty} W_{2^j}^k f(x, y) * \frac{1}{2^j} \Psi^k\left(-\frac{x}{2^j}, -\frac{y}{2^j}\right)$$

We used two orientations within the wavelet transform ($K=2$). The finite dyadic scale parameter J ($J \in \mathbb{Z}$) is the maximum scale level for a wavelet decomposition. Let's take a closer look at the transforms $W_{2^j}^1 f(x, y)$ and $W_{2^j}^2 f(x, y)$. The horizontal variations of the original image $f(x, y)$ at scale 2^j are $W_{2^j}^1 f(x, y)$. The vertical variations of $f(x, y)$ at scale 2^j are $W_{2^j}^2 f(x, y)$. We may combine $W_{2^j}^1 f(x, y)$ and $W_{2^j}^2 f(x, y)$ to obtain a concurrence of the variations in both horizontal and vertical directions for an image at each scale 2^j ,

$$W_{2^j} f(x, y) = F(W_{2^j}^1 f(x, y), W_{2^j}^2 f(x, y)) \quad k \in (1, 2),$$

where F is a combining function. The wavelet maxima for horizontal orientations $M_{2^j}^1 f(x, y)$ and vertical orientations $M_{2^j}^2 f(x, y)$ at scale 2^j are selected by the expressions below:

$$M_{2^j}^1 f(x, y) = \begin{cases} W_{2^j}^1 f(x, y) & \text{if } W_{2^j}^1 f(x, y) > W_{2^j}^1 f(x+1, y) \\ & \text{and } W_{2^j}^1 f(x, y) > W_{2^j}^1 f(x-1, y) \\ 0 & \text{otherwise} \end{cases}$$

$$M_{2^j}^2 f(x, y) = \begin{cases} W_{2^j}^2 f(x, y) & \text{if } W_{2^j}^2 f(x, y) > W_{2^j}^2 f(x, y+1) \\ & \text{and } W_{2^j}^2 f(x, y) > W_{2^j}^2 f(x, y-1) \\ 0 & \text{otherwise} \end{cases}$$

The image can be reconstructed from its two one-dimensional wavelet maxima components alone.

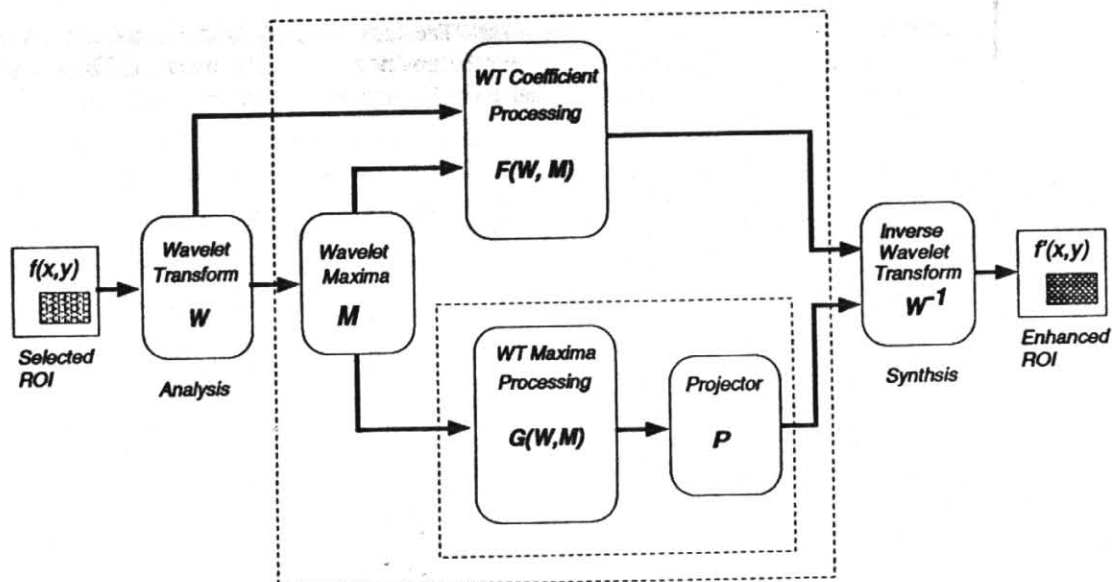


Figure 1. A framework for wavelet processing and local feature enhancement by wavelet representations.

Similar to the one-dimensional case, we may consider wavelet maxima in two-dimensions. Consider the two components of the two dimensional wavelet transform of $f(x,y)$:

$$\begin{pmatrix} W_{2^j}^1 f(x,y) \\ W_{2^j}^2 f(x,y) \end{pmatrix} = \begin{pmatrix} 2^j \frac{\partial}{\partial x} (f * \theta_{2^j}) \\ 2^j \frac{\partial}{\partial y} (f * \theta_{2^j}) \end{pmatrix} (x,y) = 2^j \nabla (f * \theta_{2^j})(x,y)$$

The modulus and angle of the gradient vector are defined respectively by

$$M_{2^j}(x,y) = \left(|W_{2^j}^1 f(x,y)|^2 + |W_{2^j}^2 f(x,y)|^2 \right)^{\frac{1}{2}}, \quad A_{2^j} f(x,y) = \arctan \left(\frac{W_{2^j}^2 f(x,y)}{W_{2^j}^1 f(x,y)} \right).$$

The gradient vector points in the direction along which the partial derivative of $f * \theta_{2^j}(x,y)$ has a maximum amplitude. At each scale 2^j , the modulus maxima of the wavelet transform are defined as points where the modulus image $M_{2^j}(x,y)$ are locally maximum along the gradient direction given by $A_{2^j}(x,y)$. Thus the wavelet transform maxima representation of an image consists of

$$\left\{ (M_{2^j} f(u_n, v_n), A_{2^j} f(u_n, v_n))_{1 \leq j \leq J, n \in \mathbb{Z}}, S_{2^j} f(x,y) \right\} \quad \text{or} \\ \left\{ (W_{2^j}^1 f(u_n, v_n), W_{2^j}^2 f(u_n, v_n))_{1 \leq j \leq J, n \in \mathbb{Z}}, S_{2^j} f(x,y) \right\},$$

where $(u_n, v_n)_{n \in \mathbb{Z}}$ are the points where $M_{2^j}(x,y)$ reach a maxima. Similar to the one dimensional case, we may reconstruct $f(x,y)$ from its two-dimensional wavelet transform maxima representation alone[22].

Wavelet representations localize mammographic features. In addition, wavelet maxima can localize image noise, which usually lies in the higher frequency bands. A problem for image enhancement in mammography is the ability to emphasize mammographic features while *reducing* the enhancement of noise. We shall show that by classifying transform coefficients and wavelet maxima, noise may be removed and mammographic features enhanced non-destructively.

Non-linear techniques for image enhancement can be applied within the context of wavelet decompositions. As shown in Figure 1, we may first select a region of interest within a digitized radiograph. Next, wavelet maxima edges are extracted from the transform coefficients. We can choose to enhance features by either the maxima coefficients alone, or by using the maxima coefficients as "pointers" into the complete transform space. Finally, we simply invert the emphasized transform coefficients or projector operators may be used to recover the enhanced image $f'(x,y)$ from weighted maxima features alone. Below we present a general formula for processing wavelet transform coefficients and maxima features respectively:

$$W_{2^j}^k f(x,y) = F(W_{2^j}^1 f(x,y), W_{2^j}^2 f(x,y), M_{2^j}^1 f(x,y), M_{2^j}^2 f(x,y)) \quad \text{or} \\ M_{2^j}^k f(x,y) = G(W_{2^j}^1 f(x,y), W_{2^j}^2 f(x,y), M_{2^j}^1 f(x,y), M_{2^j}^2 f(x,y)), \quad j \in \{0, 1, \dots, J-1\}$$

The functions F and G are user defined to emphasize certain features within a selected scale or region. We obtained enhancements from representations of both wavelet coefficients and wavelet maxima by using the inverse wavelet transform directly and by reconstruction from wavelet maxima features alone, i.e.

$$f'(x, y) = W^{-1}(W' f(x, y)),$$

$$f'(x, y) = P(M' f(x, y))$$

where P is the projection operator described earlier in section 2. By defining F and G functions we may design alternate enhancement schemes. For example, noise may be eliminated by thresholding wavelet coefficients:

$$W'_{2j} f(x, y) = \begin{cases} W_{2j}^k f(x, y) & \text{if } M_{2j}^k(x, y) < T_j \\ W_{2j}^k f(x, y) \cdot g(j) & \text{if } M_{2j}^k(x, y) \geq T_j \end{cases} \quad 1 \leq k \leq 2, j \in \{0, 1, \dots, J-1\}$$

$$f'(x, y) = W^{-1}(W'_{2j} f(x, y))$$

where T is some threshold constant, and $g(l)$ is a scale-space weighting function defined below:

$$g(l) = \begin{cases} c & \text{constant enhancement} \\ k \cdot l + c & \text{linear enhancement} \\ e^{k \cdot l + c} & \text{exponential enhancement} \\ k \cdot \ln(l) & \text{logarithmic enhancement} \end{cases}$$

The parameters c, k are small constants, and l is a selected decomposition level. To enhance features "living" in a single level or within a contiguous subset of levels, we simply modify the wavelet scale-space weight function:

$$g'(l) = \sum \delta(l - l_i) \cdot g(l_i)$$

where l_j is the level number upon which an enhancement is focused.

Alternatively we may target exactly horizontal or vertical mammographic features by using $g(l)$ to weight each distinct level j :

$$W'_{2j} f(x, y) = \begin{cases} W_{2j}^k f(x, y) & \text{if } M_{2j}^k(x, y) < T_j \\ W_{2j}^k f(x, y) \cdot g(j) & \text{if } M_{2j}^k(x, y) \geq T_j \end{cases} \quad j \in \{0, 1, \dots, J-1\}.$$

$$W'_{2j} f(x, y) = W_{2j}^{k'} f(x, y)$$

and reconstruct an enhanced image simply by

$$f'(x, y) = W^{-1}(W'_{2j} f(x, y)), \quad k \in \{1, 2\}, \quad j \in \{0, 1, \dots, J-1\}.$$

For $k=1, k'=2$, horizontal features are enhanced, and for $k=2, k'=1$, vertical features are enhanced.

When wavelet maxima representations alone are modified for feature enhancement, we apply a global threshold across all levels of the decomposition, and multiply the maxima coefficients by a similar weighting function,

$$M'_{2j} f(x, y) = \begin{cases} M_{2j}^k f(x, y) & \text{if } M_{2j}^k(x, y) \leq T \\ M_{2j}^k f(x, y) \cdot g(j) & \text{if } M_{2j}^k(x, y) > T \end{cases}$$

$$f'(x, y) = P(M'_{2j} f(x, y)) \quad j \in \{0, 1, \dots, J-1\}; \quad 1 \leq k \leq 2.$$

Similarly, we may also weight the horizontal or vertical mammographic features independently within each scale.

$$M_{2j}^{k'} f(x, y) = \begin{cases} M_{2j}^k f(x, y) & \text{if } M_{2j}^k(x, y) \leq T \\ M_{2j}^k f(x, y) \cdot g(j) & \text{if } M_{2j}^k(x, y) > T \end{cases} \quad j \in \{0, 1, \dots, J-1\}$$

$$M_{2j}^{k'} f(x, y) = M_{2j}^k f(x, y)$$

and reconstruct an enhanced image without noise by

$$f'(x, y) = P(M_{2j}^{k'} f(x, y)), \quad k \in \{1, 2\}, \quad j \in \{0, 1, \dots, J-1\}.$$

An advantage of using multiscale analysis for mammographic enhancement is that we can incrementally and selectively focus on features of mammographic interest. If the weighting function $g(l)$ is defined to enhance a single scale, then a specific focused enhancement of features is accomplished in reconstruction. We may combine any representations from any subset of scales and visualize incrementally mammographic features of specific size and/or shape.

3.1 Multiwavelet Decompositions

In the previous section, we presented methods of enhancement by weighting coefficients within distinct scales of a single wavelet decomposition. We now extend the idea to include more than one wavelet decomposition. Suppose we have a series of wavelets $\Psi_i^k(x, y)$ $i=1, 2, \dots, N$, $k=1, \dots, K$, where N is the number of distinct analyzing functions. Each analyzing function decomposes a mammogram into J distinct levels. For each wavelet Ψ_i^k we compute its decomposition for some image $f(x, y)$:

$$W_{i,2j}^k = f(x, y) * \frac{1}{2^j} \Psi_i^k\left(\frac{x}{2^j}, \frac{y}{2^j}\right), \quad k \in \{1, \dots, K\}$$

The reconstruction of $f(x, y)$ from its two-dimensional dyadic transform is accomplished by,

$$f(x, y) = \sum_{k=1}^K \sum_{j=-\infty}^{\infty} W_{i,2j}^k f(x, y) * \frac{1}{2^j} \Psi_i^k\left(-\frac{x}{2^j}, -\frac{y}{2^j}\right) \quad i \in \{1, 2, \dots, N\}.$$

The maxima (edges) of the wavelet transform coefficients are detected along the rows of $W_{i,2j}^1 f(x, y)$ and columns of $W_{i,2j}^2 f(x, y)$. Let $M_{i,2j}^1 f(x, y)$ and $M_{i,2j}^2 f(x, y)$ define the wavelet maxima of horizontal and vertical features respectively, then

$$M_{i,2j}^1 f(x, y) = \begin{cases} W_{i,2j}^1 f(x, y) & \text{if } W_{i,2j}^1 f(x, y) > W_{i,2j}^1 f(x+1, y) \\ & \text{and } W_{i,2j}^1 f(x, y) > W_{i,2j}^1 f(x-1, y) \\ 0 & \text{otherwise} \end{cases} \quad \begin{matrix} j \in \{0, 1, \dots, J-1\}, \\ i \in \{1, 2, \dots, N\}, \end{matrix}$$

$$M_{i,2j}^2 f(x, y) = \begin{cases} W_{i,2j}^2 f(x, y) & \text{if } W_{i,2j}^2 f(x, y) > W_{i,2j}^2 f(x, y+1) \\ & \text{and } W_{i,2j}^2 f(x, y) > W_{i,2j}^2 f(x, y-1) \\ 0 & \text{otherwise} \end{cases} \quad \begin{matrix} j \in \{0, 1, \dots, J-1\}, \\ i \in \{1, 2, \dots, N\}. \end{matrix}$$

Below we present a general formula to process transform and wavelet maxima representations computed from more than one analyzing function respectively,

$$W_{2j}^{k'} f(x, y) = F(W_{i,2j}^1 f(x, y), W_{i,2j}^2 f(x, y), M_{i,2j}^1 f(x, y), M_{i,2j}^2 f(x, y)) \quad \text{and}$$

$$M_{2j}^{k'} f(x, y) = G(W_{i,2j}^1 f(x, y), W_{i,2j}^2 f(x, y), M_{i,2j}^1 f(x, y), M_{i,2j}^2 f(x, y))$$

$$j \in \{0, 1, \dots, J-1\}, \quad i \in \{1, 2, \dots, N\}, \quad k \in \{1, 2\}.$$

The functions F and G are user defined to emphasize features living within a specific scale. Similarly, we may recover the enhanced image $f'(x,y)$ from the processed wavelet transform coefficients or weighted wavelet maxima coefficients by using either the inverse wavelet transform or reconstruct by projection operators for each wavelet $\Psi_i(x)$:

$$f'(x,y) = W_i^{-1}(W'_i f(x,y)) \quad \text{or} \\ f'(x,y) = P_i(M'_i f(x,y)).$$

Lets consider an example of multiwavelet enhancement. For each level of the decomposition, we define the function F to return a set of wavelet coefficients from the pool of the two original bases sets, W_1 and W_2 . For reconstruction, the new set of coefficients is treated as if it were a basis set from W_1 . Distinct wavelet maxima coefficients may be exchanged within each level of the decomposition and treated in the same way by the function G .

$$W_{1,2j}^{k'} f(x,y) = F(W_{2,2j}^1 f(x,y), W_{2,2j}^2 f(x,y)) \quad \text{or} \\ M_{1,2j}^{k'} f(x,y) = G(M_{2,2j}^1 f(x,y), M_{2,2j}^2 f(x,y)), \quad j \in \{0, 1, \dots, J-1\}, \quad k \in \{1, 2\}$$

A special case is when we define F (or G) to simply return the complete set of basis (all levels) for W_2 . In either case, a scale-space weighting function $g(l)$ may be employed to emphasize features within particular levels of a transform.

$$W_{1,2j}^{k'} f(x,y) = g(j) W_{2,2j}^k f(x,y) \quad \text{or} \\ M_{1,2j}^{k'} f(x,y) = g(j) M_{2,2j}^k f(x,y)$$

In this example, the formulas to reconstruct from the W_1 basis are simply,

$$f'(x,y) = W_1^{-1}(W'_1 f(x,y)) \quad \text{or} \\ f'(x,y) = P_1(M'_1 f(x,y)).$$

3.2 Wavelet Packet Representations

Analysis by wavelet packets, pioneered by Coifman and Wickerhauser[4], is a generalization on compactly supported wavelets[7], and has been successfully used for acoustical signal compression[5]. Wavelet packets are a collection of functions $\{W_j(x)|j \in \mathbb{Z}^+\}$ obtained by dilation and translation in the following way,

$$2^{\frac{p-1}{2}} W_{2n}(2^{p-1}x - l) = \sum_m h_{m-2l} 2^{\frac{p}{2}} W_n(2^p x - m) \\ 2^{\frac{p-1}{2}} W_{2n+1}(2^{p-1}x - l) = \sum_m g_{m-2l} 2^{\frac{p}{2}} W_n(2^p x - m)$$

where the p is a scale index and l is a translation index. $W_0(x) = \phi(x)$ is a scaling function, and $W_1(x) = \psi(x)$ is a basic wavelet described in [7][19]. The discrete filters h_k and g_k are quadrature mirror filters[6].

The inverse relationship between wavelet packets of different scales can be expressed as,

$$2^{\frac{p}{2}} W_n(2^p x - k) = \sum_l h_{k-2l} 2^{\frac{p-1}{2}} W_{2n}(2^{p-1}x - l) + \sum_l g_{k-2l} 2^{\frac{p-1}{2}} W_{2n+1}(2^{p-1}x - l).$$

This relationship allows us to accomplish reconstruction from coarse to fine scales.

Any function $f(x) \in L^2(R)$ can be decomposed into a wavelet packet basis. The coefficients of this decomposition are simply the inner product of $f(x)$ with different wavelet packets. For example, the coefficients from an inner product $\langle f(x), W_n(2^p x - k) \rangle$ indicate the intensity of this component in $f(x)$. An approximation of the function $f(x)$ at scale 2^p for wavelet packet W_n can be computed by

$$A_n^{2^p} f(x) = \sum_k S_{n,k}^{2^p} 2^{\frac{p}{2}} W_n(2^p x - k)$$

where $S_{n,k}^p = \langle f(x), 2^{\frac{p}{2}} W_n(2^p x - k) \rangle = 2^{\frac{p}{2}} \int_{-\infty}^{\infty} f(x) W_n(2^p x - k) dx$. Wavelet packet analysis provides an efficient way to compute transform coefficients. From above equation, we have

$$S_{n,k}^p = \langle f(x), 2^{\frac{p}{2}} W_n(2^p x - k) \rangle = \sum_l h_{k-2l} S_{2n,l}^{p-1} + \sum_l g_{k-2l} S_{2n+1,l}^{p-1}$$

Components of coarser scales are calculated by the formulas

$$S_{2n,l}^{p-1} = \langle f(x), 2^{\frac{p-1}{2}} W_{2n}(2^{p-1} x - l) \rangle = \sum_m h_{m-2l} S_{n,m}^p \quad \text{and}$$

$$S_{2n+1,l}^{p-1} = \langle f(x), 2^{\frac{p-1}{2}} W_{2n+1}(2^{p-1} x - l) \rangle = \sum_m g_{m-2l} S_{n,m}^p$$

and computed recursively. The complete decomposition tree is shown in Figure 2(a).

In the case of 2-D image signals, wavelet packets may be computed simply as tensor products of 1-D wavelet packets. A complete wavelet packet decomposition tree is a redundant representation. Only a subset of the coefficients are required to completely represent an image. To accomplish enhancement, we can identify a best basis for which a decomposition has fewest nonzero coefficients, and modify the coefficients within these wavelet packet nodes in the same way as standard wavelet decompositions. Figure 8 shows the first two levels of a wavelet packet decomposition of the original mammogram shown in Figure 2(c). In the next section, we present preliminary results of wavelet processing for the dense mammogram shown in Figure 2(c).

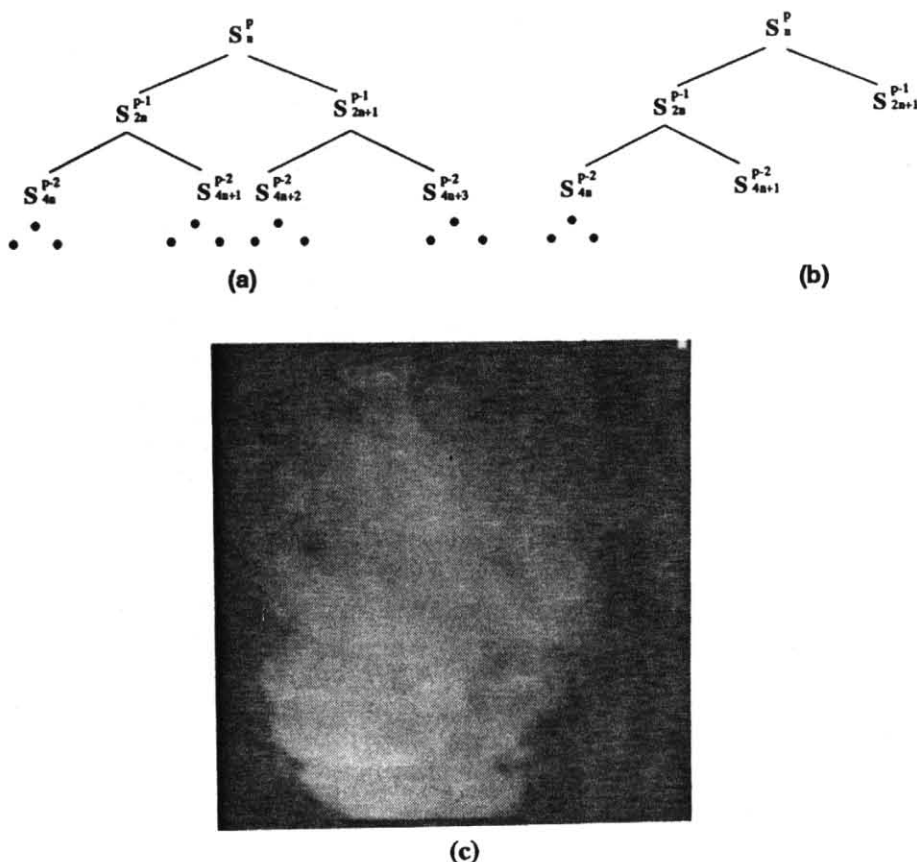


Figure 2. (a) Complete (full recursion) wavelet packet decomposition tree. (b) Standard wavelet decomposition. (c) Original dense mammogram.

4. Experimental Results

Preliminary results have shown that the wavelet processing techniques described above, can make more obvious unseen or barely seen features of a mammogram without requiring additional radiation. Our study examined reconstructions and well localized transform coefficients in scale-space obtained from several analyzing functions. Mammograms were reconstructed from their wavelet maxima representations and enhanced by linear, exponential and constant functions through scale-space using several analyzing wavelets.

In this section, we show photographs for reconstructions of a dyadic scale space. A cubic spline analyzing function[21] was used to accomplish each decomposition. The original (dense) mammogram is shown in Figure 2(c). The first three levels of the decomposition are shown in Figure 3. The left and right columns of Figure 3 show the magnitude of the horizontal and vertical projections (wavelet coefficients) within each scale, respectively. Next, Figure 4 shows the set of images used to identify two-dimensional wavelet maxima coefficients. The photographs shown in the leftmost column of Figure 4 were obtained by combining wavelet coefficients oriented along the x and y directions. Thus, a single picture is shown for each distinct level. Please note the clear geometric shape of the calcifications seen at the finer levels of the scale space. The photographs in the middle column show the orientation of the coefficients at each level. For purpose of display, the range 0 to 360 degrees has been mapped to gray scale values 0 to 255.

The wavelet maxima coefficients are shown as binary images in the rightmost column of Figure 4. As described earlier, we used this representation as an "index" for coefficient weights to emphasize significant features "living" within a level of the transform space. Thus, we accomplished various non-linear enhancements as shown in Figure 9(a). In this context, the opportunity to focus on specific features for enhancement via geometric constraints is likely to be extremely valuable. Please note that each picture shown in Figures 1 and 2 was obtained exactly from the original mammogram shown in Figure 9(b)! No new information has been added. Rather, we have selectively discarded information in each case. Figure 9(a) shows a mammogram enhanced by indexing wavelet maxima coefficients and multiplying the non-negative coefficients in the two finest levels of scale by the weights 3 and 5 respectively.

We constructed mathematical phantom models to validate our enhancement techniques against false positives arising from possible artifacts. These models included features of regular and irregular shapes and sizes of interest in mammographic imaging, such as microcalcifications, cylindrical or spiculated objects and conventional masses. Figure 5(a) shows an example of one of our mathematical phantoms.

Techniques for "blending" a normal mammogram with the images of mathematical models, were developed. The purpose of this exercise was to test our processing techniques on known inputs using mammograms where the objects of interest were deliberately obscured by normal breast tissues. The "imaging" justification for "blending" is readily apparent; a cancer is visible in a mammogram because of its (slightly) higher x-ray attenuation which causes a lower radiation exposure on the film in the appropriate region of a projected image. Figure 5(b) shows an example of a mammogram whereby the mathematical phantom shown in Figure 5(a), has been blended into the mammogram by a judicious choice of multiplication weights, adding the amplitude of the mathematical phantom image followed by local smooth filtering of the resultant combined image.

In Figure 6(a), two-dimensional wavelet edge coefficients within level two alone, were multiplied by a weight factor of 8, within a selected region of interest. Note that the dominant mass is made more visible by local emphasis at this level. In Figure 6(b) we show another enhanced mammogram containing the mathematical phantom shown in Figure 5(a). In this case, a multiwavelet technique is demonstrated. The improved visibility of the microcalcifications (input objects) shown in Figure 7, clearly illustrates the potential of wavelet analysis to enhance the visibility of objects of interest to mammography.

The first two levels of a wavelet packet decomposition are shown in Figure 8. Wavelet representations may be likewise identified from each of the subsquares shown and retained to emphasize features within each scale.

Acknowledgements: This work was sponsored in part by the Department of Radiology at the University of Florida, Gainesville. The authors wish to thank Edward Staab, Janice Honeyman, Barbara Steinbach, Walter Huda and Bjorn Jawerth for their support and encouragement.

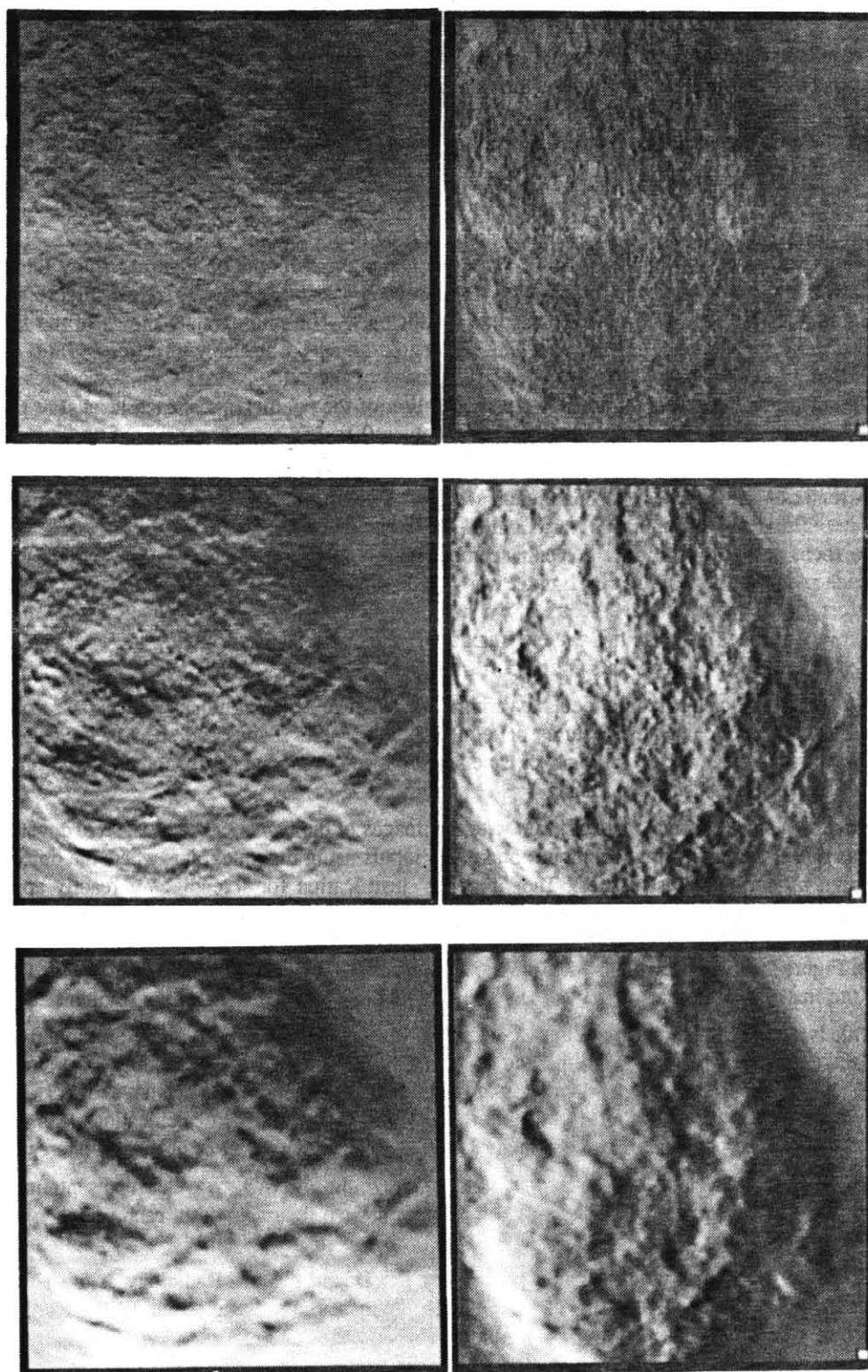


Figure 3. Magnitude of wavelet coefficients for horizontal and vertical orientations, levels 1, 2 and 3.

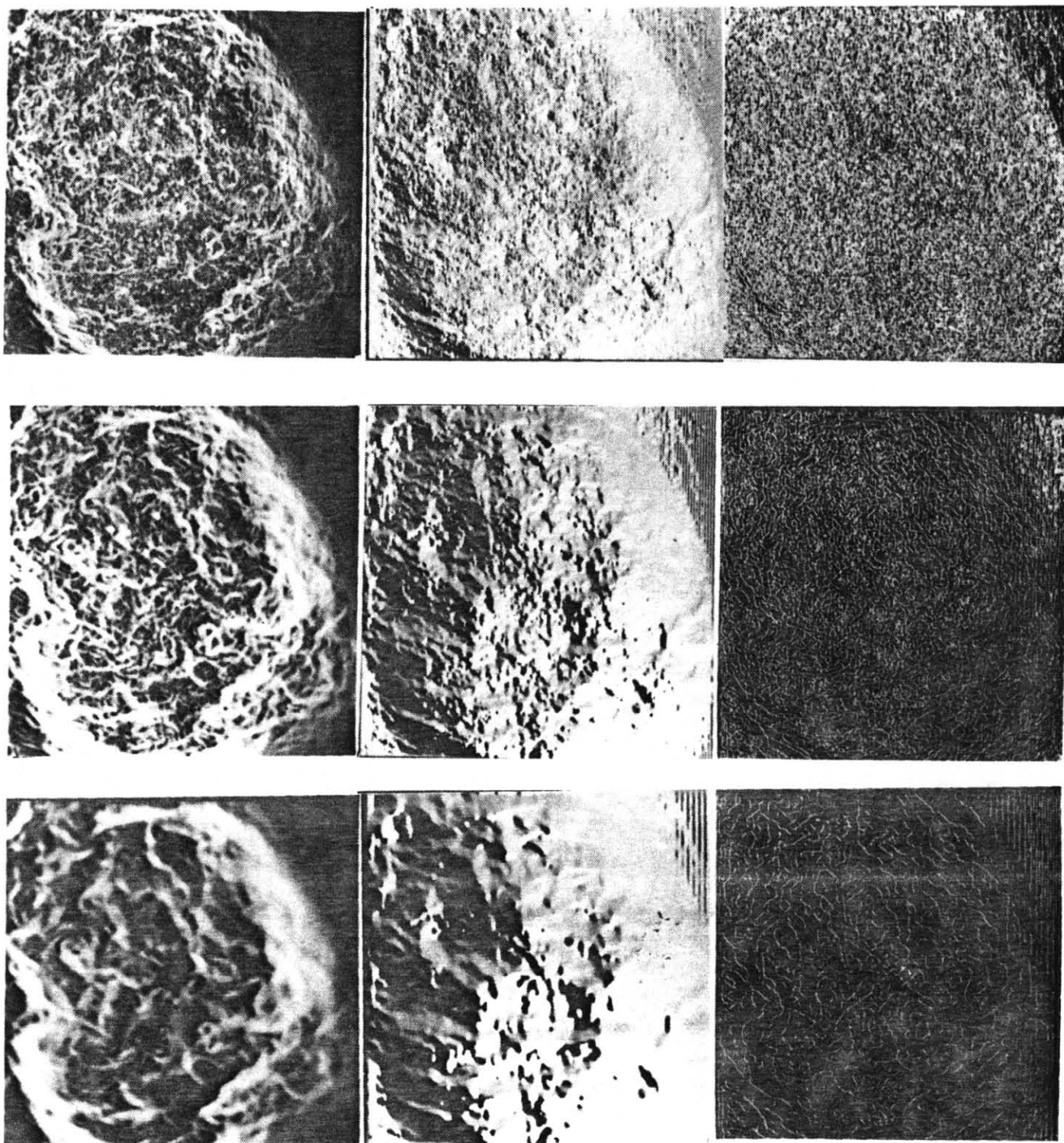
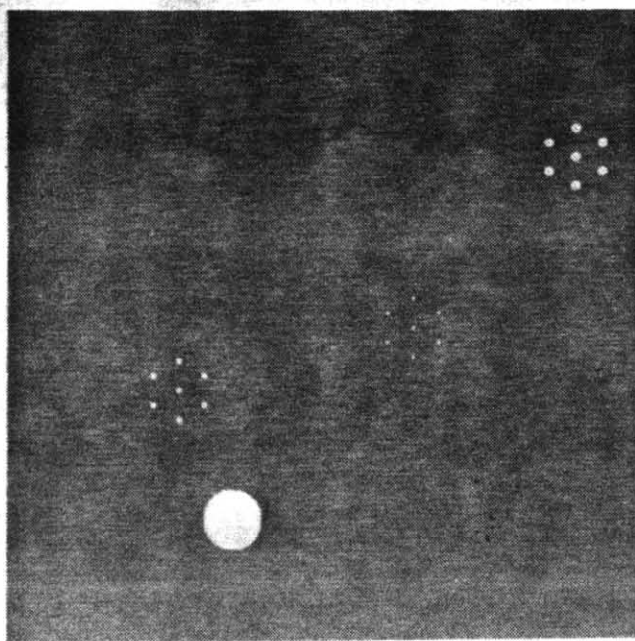
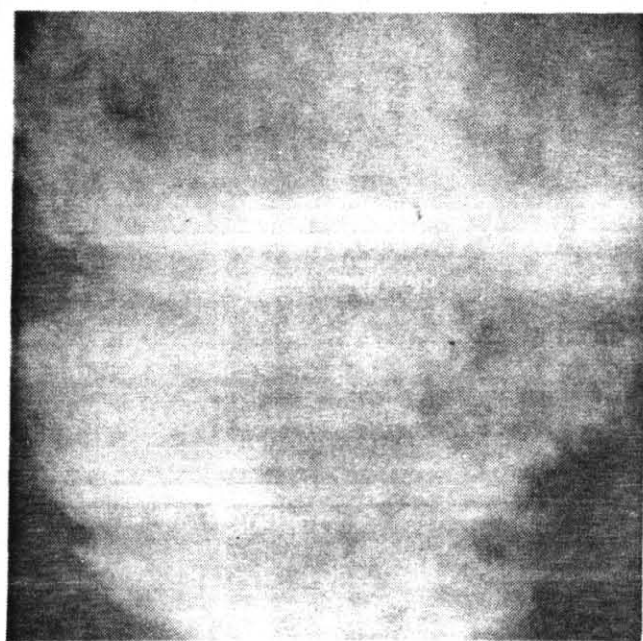


Figure 4. The leftmost column shows the combination of horizontal and vertical orientations of the wavelet coefficients at scales 1,2 and 3 respectively. The center column shows the directions of the combined coefficients. The two-dimensional wavelet maxima for levels 1, 2 and 3 are shown as binary edges in the rightmost column.

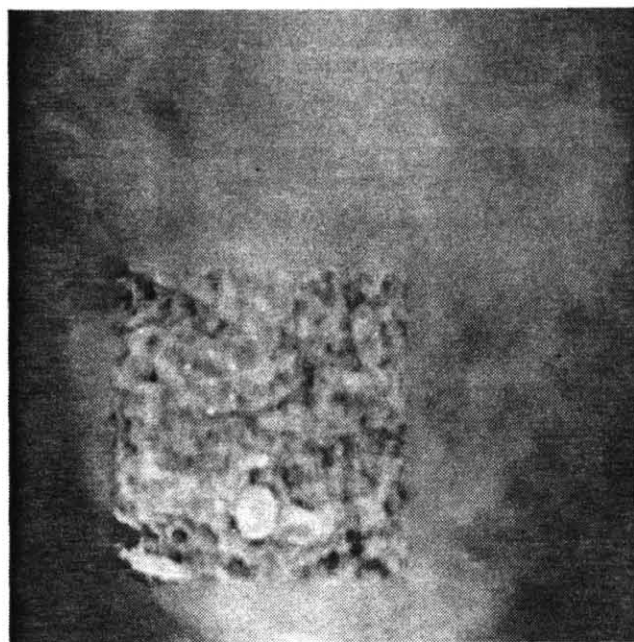


(a)

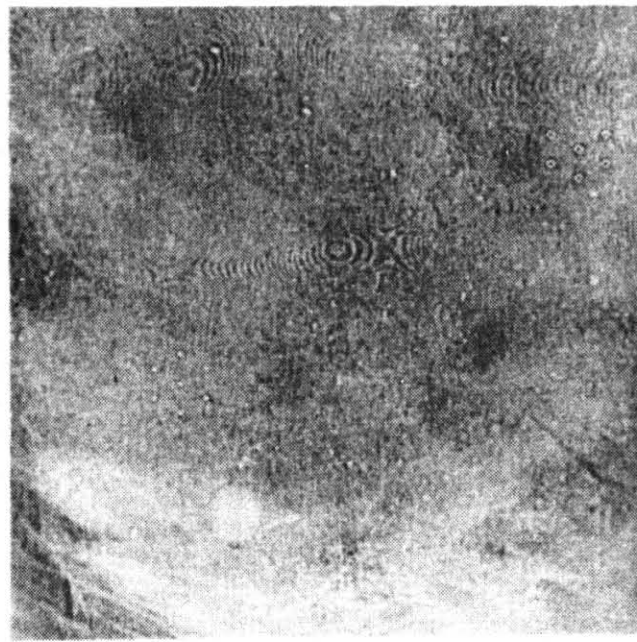


(b)

Figure 5. (a) Mathematical phantom of mammographic features. (b) Original mammogram blended with the mathematical phantom.



(a)



(b)

Figure 6. (a) ROI enhancement by emphasizing the maxima coefficients on level 2 alone. (b) Enhancement by a multiwavelet decomposition.

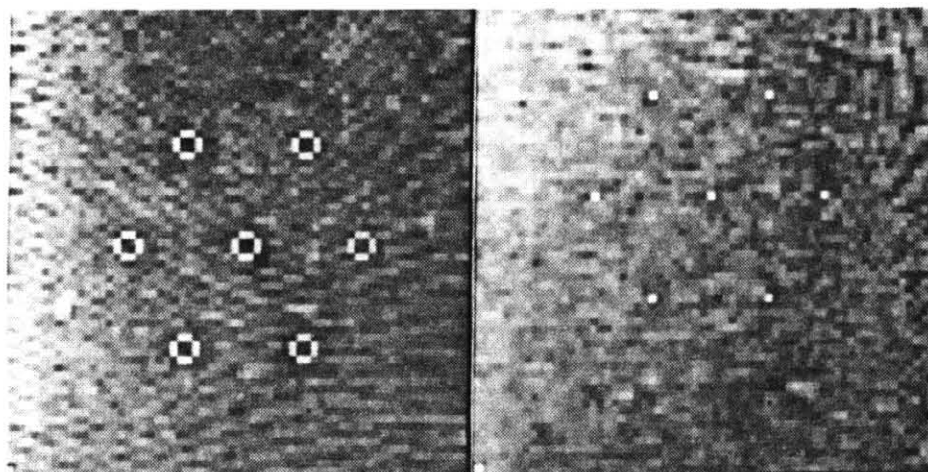


Figure 7. Local enlargement (16X) of the enhanced calcifications shown in Figure 6.

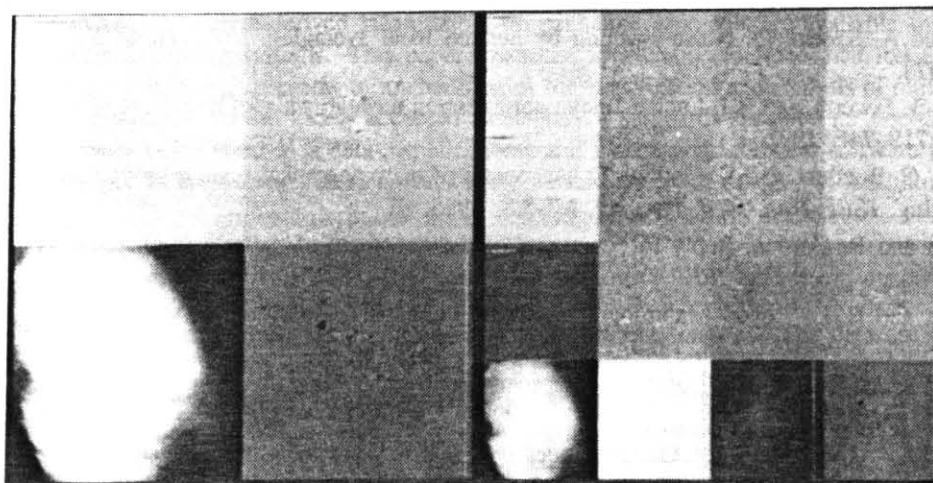


Figure 8. A wavelet packet decomposition, levels 1 (left) and 2 (right).

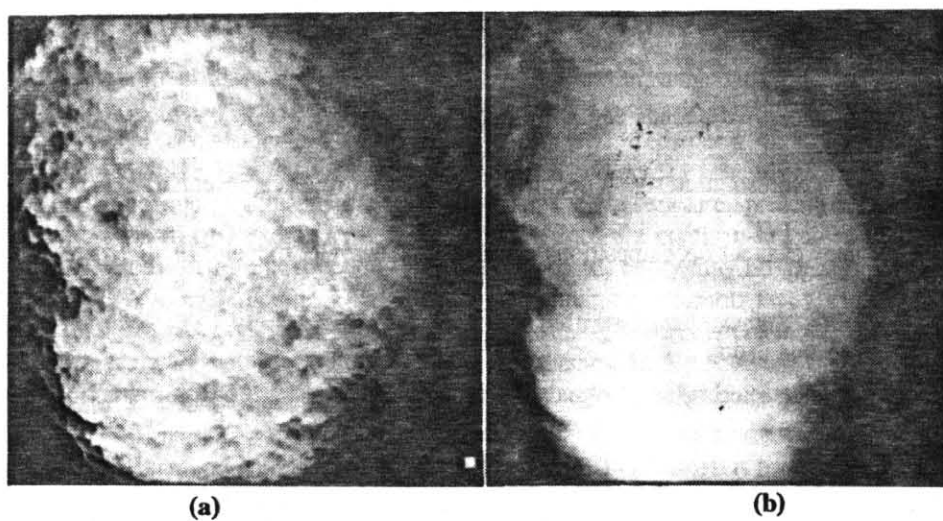


Figure 9. (a) A nonlinear enhancement. (b) Original dense mammogram.

References

- [1] A.C. Bovik, T. S. Huang, and D. C. Munson. The effect of median filtering on edge estimation and detection. *IEEE Trans. Pattern Anal. Machine Intell.*, PAMI-9:181-194, 1987.
- [2] D. Brzakvoic, X. M. Luo, and P. Brzakvoic. An approach to automated detection of tumors in mammograms. *IEEE Trans. Med. Imaging*, MI-9(3):233-241, 1991.
- [3] F. Campbell and J. Kulikowski. Orientation selectivity of the human visual system. *Journal of Physiology*, 197:437-441, 1966.
- [4] R. R. Coifman and Y. Meyer. Orthonormal wave packet bases. *preprint, Yale Univ.*, 1989.
- [5] R. R. Coifman and M.V. Wickerhauser. Entropy-based algorithms for best basis selection. *IEEE Trans. on Info. Theory*, 38(2):713-718, 1992.
- [6] R.E. Crochiere and L.R. Rabiner. *Multirate Digital Signal Processing*. Prentice-Hall, 1983.
- [7] I. Daubechies. Orthonormal bases of compactly supported wavelets. *Communications on Pure and Applied Mathematics*, XLI:909-1005, 1988.
- [8] I. Daubechies. The wavelet transform, time-frequency localization and signal analysis. *IEEE Trans. on Info. Theory*, 36(5):961-1005, 1990.
- [9] L. S. Davis and A. Rosenfield. Noise cleaning by iterated local averaging. *IEEE Trans. Syst., Man, Cybern.*, SMC-8:705-710, 1978.
- [10] R. A. Devore, B. Jawerth, and B.J. Lucier. Image compression through wavelet transform coding. *IEEE Trans. on Info. Theory*, 38(2):719-746, 1992.
- [11] A. P. Dhawan, G. Buelloni, and R. Gordon. Enhancement of mammographic feature by optimal adaptive neighborhood image processing. *IEEE Tran. Med. Imaging*, MI-5:8, 1986.
- [12] A. P. Dhawan and R. Gordon. Reply to comments on enhancement of mammographic feature by optimal adaptive neighborhood image processing. *IEEE Trans. Med. Imaging*, MI-6:82, 1987.
- [13] A. P. Dhawan and E. Le Royer. Mammographic feature enhancement by computerized image processing. *Comput. Methods Programs Biomed.*, 27:23, 1988.
- [14] R. Gorden and R. M. Rangayyan. Feature enhancement of film mammograms using fixed and adaptive neighborhoods. *Appl. Opt.*, 23:560, 1984.
- [15] S. M. Lai, X. Li, and W. F. Bischof. On techniques for detecting circumscribed masses in mammograms. *IEEE Trans. Med. Imaging*, MI-8(4), 1989.
- [16] A. Laine. Multiscale wavelet representations for mammographic feature analysis. In *Image Enhancement Techniques: Computer Science, National Cancer Institute Breast Imaging Workshop: State-of-the-Art and New Technologies*, September 5, 1991, Bethesda, MD.
- [17] P. G. Lemarie and Y. Meyer. Ondelettes et bases hilbertiennes. *Revista Mathematica Ibero Americana*, 2, 1986.
- [18] S. Mallat. Multiresolution approximations and wavelet orthonormal bases of $l(r)$. *Trans. Amer. Math. Soc.*, 315(1):69-87, 1989.
- [19] S. Mallat. A theory for multiresolution signal decomposition: The wavelet representation. *IEEE Transactions on PAMI*, 11(7):674-693, 1989.
- [20] S. Mallat. Timefrequency channel decompositions of image and wavelet models. *IEEE Trans. ASSP*, 37(12):891-896, 1989.
- [21] S. Mallat and S. Zhong. Signal characterization from multiscale edges. In *10th International Conf. on Pattern Recognition*, pages 891-896, 1990.
- [22] S. Mallat and S. Zhong. Characterization of signals from multiscale edges. *IEEE Trans. on PAMI*, 14(7):710-732, 1992.
- [23] M. Nagao and T. Matsuyama. Edge preserving smoothing. *Computer Graphics and Image processing*, 9:394-407, 1979.
- [24] A. Scheer, F.R.D. Velasco, and A. Rosenfield. Some new image smoothing techniques. *IEEE Trans. Syst., Man, Cybern.*, SMC-10(3):153-158, 1980.
- [25] P. G. Tahoces, J. Correa, M. Souto, C. Gonzalez, L. Gomez, and J. Vidal. Enhancement of chest and breast radiographs by automatic spatial filtering. *IEEE Trans. Med. Imaging*, MI-10(3):330-335, 1991.